Check for updates

Epitaxial growth and magnetic/transport properties of La$_{0.7}$Sr$_{0.3}$MnO$_3$ thin films grown on SrTiO$_3$ with optimized growth conditions

K. Wang,[ab] M. H. Tang, [iD] *[ab] Y. Xiong,[c] G. Li,[ab] Y. G. Xiao,[ab] W. L. Zhang,[ab] Z. P. Wang,[d] Z. Li*[ab] and J. He[e]

Epitaxial growth of colossal magnetoresistive thin films of La$_{0.7}$Sr$_{0.3}$MnO$_3$ (LSMO) has been achieved on TiO$_2$-terminated (001) SrTiO$_3$ (STO) single-crystal substrates using PLD (pulsed laser deposition). The temperature dependence of film magnetization and resistance was measured and the characteristics of film surface roughness were studied. Effects of oxygen partial pressure and substrate temperature on the surface topography, Curie temperature (T_C) and metal–insulator transitions (T_{MI}) were also investigated. It has been found that oxygen partial pressure has more influence on the Curie temperature but less on the surface topography than the substrate temperature does. Meanwhile, at high oxygen partial pressures, Curie temperatures of sample films were affected insignificantly by the substrate temperature, while the surface morphology was affected remarkably. The influence of the substrate temperature on the T_{MI} is similar to that of the Curie temperature. Finally, thin films were successfully grown with bulk-like Curie temperature of about 360 K, and a relatively high magnetization of about 1.6 $\pm$ 0.11 μ_B per Mn atom at room temperature was achieved. The surface roughness of these thin films is about 350 pm, which is close to the thickness of a layer of cells. The high quality of LSMO films was confirmed by a 10 h retention test of ultra-thin BaTiO$_3$ (BTO) films grown on La$_{0.7}$Sr$_{0.3}$MnO$_3$.

Introduction

Colossal magnetoresistance (CMR) is a very attractive material for spintronics and it has many potential applications in various fields such as magnetic field inductor, magnetic random access memory and magnetoelectric components.[1–3] La$_{0.7}$Sr$_{0.3}$MnO$_3$ (LSMO) is a prominent member of CMR, belonging to the family of typical perovskite oxides with excellent magnetic and magnetotransport properties. In view of the suitability of closely lattice-matched perovskite oxides, it is a kind of ideal material for the growth of the heteroepitaxial family analogous to compound semiconductors with high and different coupling degrees of freedom.[4,5] Compared with the conventional oxide-based magnetic materials, LSMO has outstanding half-metallic ferromagnetism[6] and relatively high Curie

temperature ($T_C \sim 369$ K).[7] Its electrode spin polarization can reach at least 95%, and a magnetoresistance ratio of more than 1800% is obtained at 4 K.[8] This makes it possible to achieve multiferroic tunnel junctions at room temperature as compared to those reported at extremely low temperatures.[9–11] Also LSMO has been widely used for giant tunnelling magnetoresistance in magnetic tunnel junctions,[8–12] and as efficient spin injection in organic spin valves.[13–18] For the synthesis of thin LSMO films, pulsed laser deposition (PLD) is considered a promising way to achieve high quality films with atomic scale variations.[19–22] For highly correlated oxide materials, interesting magnetic and electron transport properties of LSMO are closely related to the spin–lattice–charge couplings, which are very sensitive to the film thickness, stress, and growth conditions.[22,23] Structural, magnetic and transport properties of LSMO made at condition of relatively low oxygen concentrations have been studied systematically.[24–26] However, effects of high oxygen partial pressure, substrate temperature and film thickness (over one hundred monolayers thickness films (MLs)) are rarely reported. These effects can be significant on the Curie temperature and surface morphology of thin LSMO films.

In this paper, we report the effects of oxygen partial pressure and substrate temperature on properties of thin LSMO films grown on STO (001) single crystal substrates etched by a solution composed of NH$_4$F and HF. These properties include the surface roughness, Curie temperature, resistivity, and metal–

[a]Key Laboratory of Key Film Materials & Application for Equipments (Hunan Province), School of Materials Science and Engineering, Xiangtan University, Xiangtan, Hunan, 411105, China. E-mail: mhtang@xtu.edu.cn; zhengli@xtu.edu.cn

[b]Hunan Provincial Key Laboratory of Thin Film Materials and Devices, School of Materials Science and Engineering, Xiangtan University, China

[c]The School of Mathematics and Computational Science, Xiangtan University, Xiangtan, Hunan, 411105, China

[d]School of Automotive Engineering, Weifang University of Science and Technology, Weifang, Shandong, 262700, China

[e]Pacific Geoscience Centre, Geological Survey of Canada, 9860 West Saanich Road, Sidney, British Columbia, Canada V8L 4B2

insulator transition point. Our experiments suggest that it is possible for LSMO to meet requirements of the growth of epitaxial films and the fabrication of multiferroic tunnel junctions at room temperature.

Experimental

Synthesis and characterization

$La_{0.7}Sr_{0.3}MnO_3$ (LSMO) thin films were fabricated on $SrTiO_3$ (001) single-crystal substrates (5 mm × 5 mm × 0.5 mm in size) by using a PLD with a 248 nm KrF excimer laser. In order to eliminate the objective effect of the surface roughness in STO substrates, STO substrates were treated with a solution mixture of NH_4F and HF in an ultrasonic vessel for 45 s as suggested in the literature.[27] Then they were annealed at a temperature of 950 °C for 75 minutes in a tube annealing furnace with continuous oxygen injection, prior to the deposition of thin LSMO films. In this way, we can obtain typically an atomically flat, TiO_2-terminated STO (001) single-crystal substrate. The LSMO target is then pre-sputtered with about 3000 pulses right before the PLD deposition of LSMO onto a STO substrate. For experiments of testing the effects of oxygen partial pressure, the oxygen partial pressure was varied from 0.001 to 0.4 mbar while the substrate temperature was maintained at 750 °C during the PLD. The laser energy density was between 0.9 J cm^{-2} and 1 J cm^{-2} with a repetition rate of 2 Hz and a pulse duration of 20 ns. The distance between the target and substrate was about 50 mm. After the PLD deposition of LSMO thin films, samples were annealed for about 30 minutes in the PLD chamber under the original growth oxygen partial pressure to improve the oxidation quality. Under these conditions a deposition rate of 0.4 Å with each 45 pulses was determined. The thickness of the as-deposited thin films is about 50 nm. In another set of PLD depositions, substrate temperatures were varied from 650 to 850 °C while the oxygen partial pressure was kept at 0.3 mbar, and the laser energy, frequency and the distance between the substrate and target remained the same as before. Temperature dependence of the magnetization was measured by a superconducting quantum interference device (SQUID) designed and manufactured by Quantum Design. The temperature range of SQUID is from 2 to 400 K. Surface morphology of STO substrates and epitaxially grown LSMO thin films were characterized at room temperature by an atomic force microscopy (AFM) operated in contact mode. Magnetization and transport measurements were performed using a Quantum Design physical property measurement system (PPMS) in the range of 2 to 400 K.

Results and discussion

$SrTiO_3$ is a common substrate material with a lattice constant of 3.905 Å. The lattice constant of LSMO is 3.88 Å, so the lattice-misfit between $SrTiO_3$ and LSMO is (3.905–3.88)/3.905 = 6.4‰, suitable for many lattices of perovskite materials. $SrTiO_3$ is usually manufactured to single-crystal ingots through the pulling method. $SrTiO_3$ wafers can be produced in volume with slicing, polishing, and other processes due to the current maturity of wafer technologies. It is known that a STO substrate

can be treated into a TiO_2-terminated one with solution mixed with NH_4F and HF.[27] Fig. 1(a) and (b) show the AFM images of non-etched STO substrate surface topography and a typical etched STO substrate, respectively. Clear atomic steps emerge on the etched STO substrate surface. Fig. 1(c) demonstrates the AFM image of the surface morphology of a $SrTiO_3$ substrate treated by corrosion solution mixed with NH_4F and HF. Fig. 1(d) displays an AFM line cut (along the red line marked across the steps in Fig. 1(c)). From Fig. 1(d) we can clearly see that the atomic step is ∼0.4 nm, which is about the thickness of a layer of cells. The atomic terrace width is about 0.4 μm. This implies that the annealed substrate can meet the requirements of high quality epitaxial films growth.

Oxygen partial pressure is an important factor for the growth of thin LSMO films in controlling the size of crystalline grain and surface stress distribution. Fig. 2(a) shows the AFM surface images of samples grown at various oxygen partial pressures of 0.001, 0.01, 0.1, 0.2, 0.3 and 0.4 mbar, with the substrate temperature kept at 750 °C. Small particles were observed on surfaces of samples grown at 0.001 mbar. However, surfaces of samples became more flat as oxygen partial pressure was increased to 0.2 mbar. Small particles emerged again on the surface of a sample grown at 0.3 mbar. For a sample grown at 0.4 mbar, relatively big island-like particles appeared on the surface. Fig. 2(b) shows the corresponding surface roughness of samples grown at different oxygen partial pressures. As indicated in Fig. 2(b), the surface roughness of samples first decreases and then increases with the oxygen partial pressure. This is because at low oxygen partial pressures, oxygen concentration is relatively small so the blocking effect of oxygen molecules on target material gasified by the laser is weak. The speed of laser gasification of target, and that of particles hitting on to the substrate are fast, making it easy to form small particles on the substrate surface. As the oxygen partial pressure
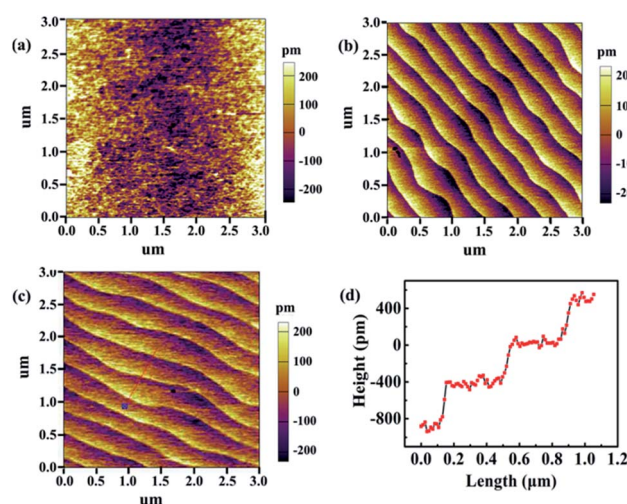

Fig. 1 (a) AFM image of not etched surface topography of the STO substrate (b) AFM image of a typical STO substrate after etched with solution composed with NH_4F and HF (c) AFM image of surface morphology of the treated $SrTiO_3$ substrate with a red line across the steps (d) an AFM line cut across the terraces in (c).
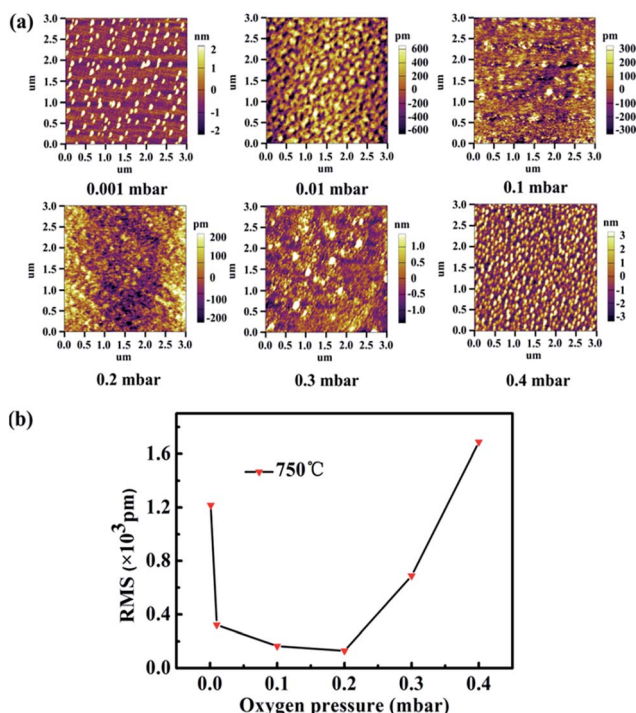
Fig. 2 (a) AFM image of LMSO films in different oxygen partial pressure. (b) The curve of root-mean-square roughness changes with oxygen partial pressure.
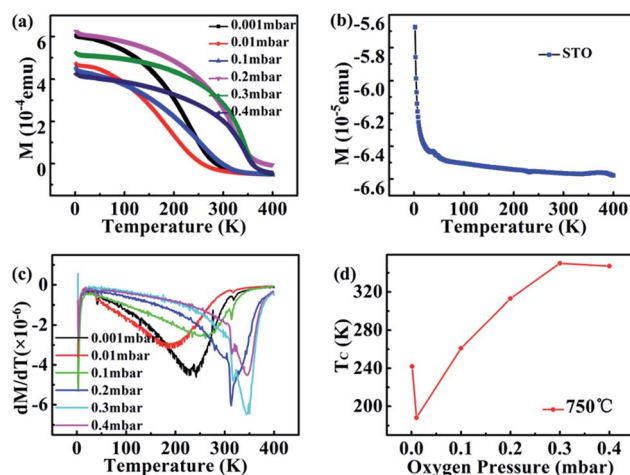

Fig. 3 (a) Temperature dependence of the magnetization with different oxygen partial pressure. (b) Temperature dependence of the magnetization of the STO substrate. (c) Derivatives of magnetization (dM/dT) of the samples. (d) The curve of Curie temperature changing with different oxygen pressure.

increases, the blocking effect of the oxygen molecules is strengthened and the deposition rate and growth mode likely reach an ideal state, leading to a flat surface. At high oxygen pressures, however, the formation of crystal nucleus becomes violent, eventually leading to large island-like particles on the surface. If one just grows a few layers of LSMO, under an appropriate oxygen partial pressure, one can reach a process that is more suitable to epitaxial growth.[20,28]

After measurements of effects of oxygen partial pressure on the surface morphology, the effect of oxygen pressure on the Curie temperature transition point was also investigated. Fig. 3(a) presents the dependence of sample magnetization on the measurement temperature ranging from 2 to 400 K for samples grown under different growth oxygen partial pressures. As shown in Fig. 3(a), negative magnetic moments are observed and the curve becomes horizontal at high measurement temperatures, which is rare for LSMO in theory. It is possible that the STO substrate has a diamagnetic moment. In fact, the magnetization of a STO substrate, as test results shown in Fig. 3(b), is negative and has a value in the same order of magnitude corresponding to those negative magnetic moments shown in Fig. 3(a). This suggests that the negative magnetic moments in Fig. 3(a) come from STO substrates. Meanwhile the magnetization still exists at a temperature of 350 K, which is better than those samples within 70 monolayers (MLs) reported previously,[19] indicating the relatively thick film would have stronger magnetism retention. In order to show the relationship between the Curie temperature and oxygen partial pressure, we calculated the derivative of magnetization (dM/dT) and define

its minimum as the Curie temperature transition point (T_C). Derivatives of magnetization (dM/dT) of these thin LSMO films are shown in Fig. 3(c). The curve of Curie temperature transition point as a function of the oxygen partial pressure is showed in Fig. 3(d). It can be observed that the values of T_C of thin LSMO films decrease at first and then increase and approaches the bulk Curie temperature of ~369 K as the growth oxygen partial pressure varies from 0.001 to 0.4 mbar. Particularly, at a growth oxygen partial pressure of 0.3 mbar, the Curie temperature is 356 K that is close to value of bulk Curie temperature of ~369 K. This is consistent with results reported in literature.[29] Although the quality of the film surface is the best at a growth oxygen partial pressure of 0.2 mbar, when take the Curie temperature into account, we still choose 0.3 mbar as the fixed value of oxygen partial pressure in the study of sample growth dependence on the substrate temperature (during PLD deposition).

Surface topography and Curie temperature transition point were investigated for different substrate temperatures ranging from 650 to 850 °C at a temperature step of 50 °C. LSMO thin films we studied were deposited at an oxygen partial pressure of 0.3 mbar using a PLD. Parameters of the pulsed laser used in our PLD are such that (1) laser energy density is between 0.9 J cm^{-2} and 1 J cm^{-2}, (2) laser frequency is 2 Hz, and (3) laser duration is 20 ns. As shown in Fig. 4(a)–(e), changes of sample surface morphology are small when the substrate temperature is below 750 °C, but particles emerged and became large when the substrate temperature is about 800 °C. Fig. 4(f) shows that the root-mean-square of surface morphology is smaller than 750 pm for samples grown at substrate temperatures ranging from 650 to 750 °C. A big step-like change is observed in sample surface roughness for samples grown at substrate temperatures between 750–800 °C. It was found that the minimum and maximum of surface roughness were about 350 pm and 2.5 nm, respectively. A possible cause for small sample roughness is that when the oxygen partial pressure is relatively high and the
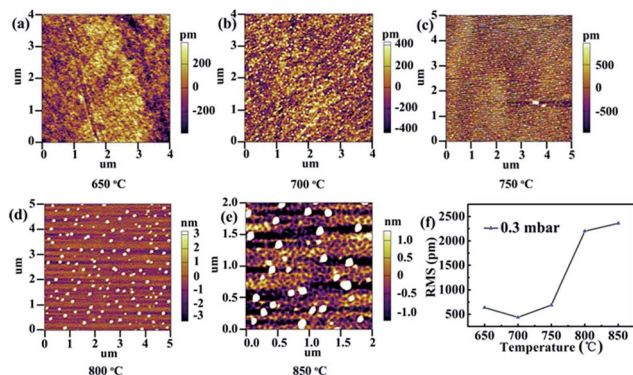
Fig. 4 (a)–(e) AFM image of LSMO films under different substrate temperature (f) the curve of root-mean-square roughness changes with substrate temperature.

substrate temperature is relatively low, the growth of LSMO films is in the layer-by-layer growth mode. Therefore, even we grow a LSMO film as thick as 50 nm, the surface of the film is still flat. However for LSMO films grown at high substrate temperatures, the formation of crystal nucleus becomes violent during the growth process and the growth mode changes from layer-by-layer to island growth. So particles emerge and film surfaces become rough. It can be seen from Fig. 5(a) that as substrate temperature increases, magnetizations of thin LSMO films decrease in the substrate temperature range of 650 to 750 °C, and they increase suddenly in the substrate temperature range of 800 to 850 °C for measurement temperature ranging from 2 to 300 K. It was observed that magnetization curves of samples grown at substrate temperature of 800 and 850 °C were overlapped, which indicates that the magnetization does not change any more in this temperature range and a saturation with substrate temperature is likely reached. A small difference of magnetization was also observed for measurement temperature varying from 300 to 400 K. As shown in Fig. 5(b), insignificant influence of the substrate temperature on the Curie temperature transition points was found, as all Curie temperatures are close to the value of 365 K.

Electron transport properties of these epitaxially grown LSMO films were measured in a closed-cycle refrigerator system or a Quantum Design physical property measurement system (PPMS) with measurement temperatures ranging from 2 to 400 K. As shown in Fig. 6(a), the resistivity difference is small for
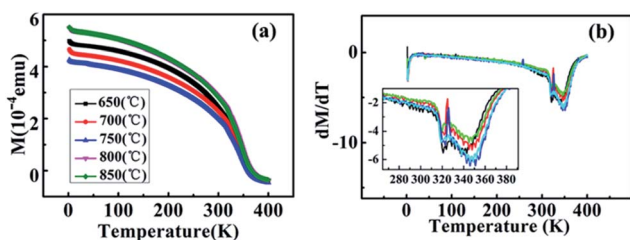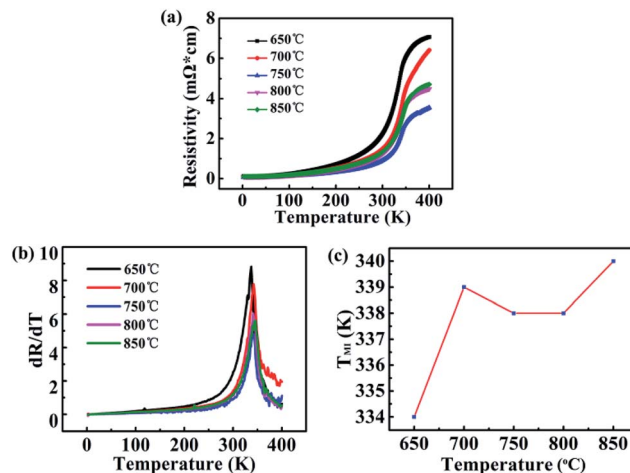

Fig. 6 (a) Measurement temperature dependence of resistivity under different substrate growth temperatures. (b) The derivatives of resistivity (dR/dT) of the samples. (c) T_{MI} as a function of the substrate growth temperature.

measurement temperatures in the range of 2 to 100 K but it becomes big for high measurement temperatures in the range of 200 to 400 K, which is consistent with results reported previously.[23] Furthermore, a more stable region appeared after 350 K for samples grown at different substrate temperatures. Overall, we found that film resistance decreased first and then increased with the substrate growth temperature. A minimum value of resistance was achieved for the substrate growth temperature of 750 °C. Meanwhile it was found that over one hundred MLs thick LSMO films have higher metal–insulator transition point and smaller resistivity as compared to those of under 20 MLs thick LSMO films as reported previously.[28] The overlapping curves corresponding to substrate growth temperatures of 800 and 850 °C are similar to the case of M–T patterns as shown in Fig. 5(a). Similarly, in order to demonstrate the relationship between the metal–insulator transition point (T_{MI}) and substrate growth temperature, we define the minimum of the derivative of resistance (dR/dT) as the metal–insulator transition point. Derivatives of resistances (dR/dT) of these thin LSMO films are showed in Fig. 6(b). The curve of T_{MI} as a function of the substrate growth temperature is presented in Fig. 6(c). From Fig. 6(b) we can see that the influence of the substrate growth temperature on the transition point of LSMO (T_{MI}) is relatively small, which is similar to its effects on Curie temperature, with T_{MI} values grouping in the range of 330–340 K as shown in Fig. 6(c).

Finally, we further grew 6 monolayers (MLs) $BaTiO_3$ (BTO) film on a $La_{0.7}Sr_{0.3}MnO_3$ substrate and tested the retention of the BTO film for 10 hours. We applied a +3 V voltage in the left section and a −3 V voltage in the right one. As can be seen in Fig. 7, the BTO ferroelectric domain stayed for 10 h. Two polarization states were clearly distinguishable in phase diagram and the black line still existed in the amplitude figure after 10 hours, indicating the polarization border areas still exist. As we know the surface morphology of thin films is significant to the growth of epitaxial heterojunction, especially

Fig. 5 (a) Temperature dependence of the magnetization with different substrate temperature. (b) Derivatives of magnetization (dM/dT) of these thin LSMO films.
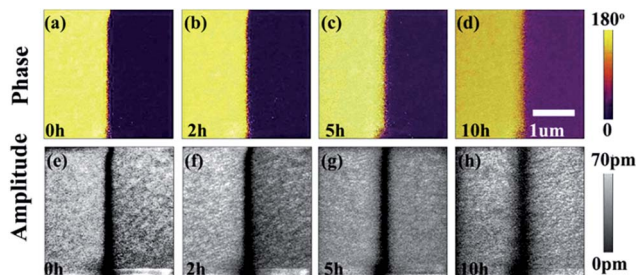
Fig. 7 (a)–(d) The phase image of BTO (e)–(h) the amplitude image of BTO. The image is 3×3 μm.

for ultrathin films such as the ferroelectric layer in ferroelectric tunnel junction. Our good results of the 10 h retention test of BTO indicate high quality of the LSMO interface. This is important for the application of BTO to ferroelectric tunnel junctions and multiferroelectric tunnel junctions.

Conclusions

In this work, STO substrates were treated into TiO_2-terminated with solution mixed with NH_4F and HF. The effect of original surface morphology, and effects of different oxygen partial pressures and different substrate temperatures on the magnetic and transport properties of $La_{0.7}Sr_{0.3}MnO_3$ (LSMO) were studied systematically. It was found that oxygen partial pressure has more influence on the Curie temperature but less influence on the surface topography than the substrate growth temperature does. Particularly, for a oxygen partial pressure of 0.3 mbar, Curie temperatures of thin films were close to the value of bulk Curie temperature ($T_C \sim 369$ K). Meanwhile we found that thicker LSMO films of about 50 nm had higher magnetization retention than thinner films reported previously when the measurement temperature is above 350 K.[19] The substrate growth temperature barely has effects on the T_C transition point and T_{MI} transition point, which suggests that if we determine the Curie temperature or metal–insulator transition point in some growth conditions, we can improve the quality of LSMO films by changing the substrate growth temperature to reduce the workload of exploring. Although 3D island growth occurs at high oxygen partial pressure and high substrate growth temperature, which indicates that strain relaxation was occurred, we found that the Curie temperature transition point and the metal–insulator transition point is almost unaffected by the substrate growth temperature. So lattice-strain probably doesn't have influence on T_C and metal–insulator transition point. However the magnetization of samples grown at high oxygen partial pressures and high substrate growth temperatures are large, so the lattice-strain relaxation may strengthen the magnetic properties. Surface morphology's become flat and have high Curie temperatures for LSMO films grown under high oxygen partial pressures and at low substrate growth temperatures during PLD process. In tests of electronic transport properties of these epitaxially grown LSMO films, it has been found that thicker LSMO films have relatively lower resistivity as compared to those within 20 MLs reported previously.[29]

Meanwhile, we further found that substrate growth temperature had a similar effect on the Curie temperature and metal–insulator transition. Furthermore, we grew 6 MLs $BaTiO_3$ (BTO) film on the $La_{0.7}Sr_{0.3}MnO_3$ substrate and the BTO have 10 hours of retention, which demonstrates the high quality of LSMO films. Finally, we successfully grew LSMO films at an optimum oxygen partial pressure to obtain a magnetization of 1.6 ± 0.11 μ_B per Mn atom at room temperature and a root-mean-square roughness of about 350 pm, which makes it possible to meet the requirement of epitaxial films and multiferroic tunnel junctions at room temperature.

Acknowledgements

Notes and references

1 A. Moreo, S. Yunoki and E. Dagotto, *Science*, 1999, **283**, 2034.
2 M. B. Salamon and M. Jaime, *Rev. Mod. Phys.*, 2001, **73**, 583.
3 E. Dagotzto, T. Hotta and A. Moreo, *Phys. Rep.*, 2001, **344**, 153.
4 See for example, D. G. Schlom, C. D. Theis and M. E. Hawley, *J. Am. Ceram. Soc.*, 1998, **86**, 41.
5 See for example, W. Eerenstein and N. D. Mathur, *Nature*, 2006, **442**, 759.
6 J. H. Park, E. Vescovo, H.-J. Kim, C. Kwon, R. Ramesh and T. Venkatesan, *Nature*, 1998, **392**, 794; Z. Y. Lu, C. H. Yang, G. D. Hu, J. C. Wang and X. Wang, *J. Alloys Compd.*, 2010, **508**, 106.
7 A. Urushibara, Y. Moritomo, T. Arima, A. Asamitsu, G. Kido and Y. Tokura, *Phys. Rev. B: Condens. Matter Mater. Phys.*, 1995, **51**, 14103.
8 M. Bowen, M. Bibes, A. Barthelemy and J.-P. Contour, *Appl. Phys. Lett.*, 2003, **82**, 2.
9 D. Pantel, S. Goetze, D. Hesse and M. Alexe, *Nat. Mater.*, 2012, **11**, 1038.
10 V. Garcia and M. Bibes, *Nat. Mater.*, 2014, **5**, 4289.
11 R. Laiho, P. Laukkanen, I. J. Vayrynen and H. S. Majumdar, *Appl. Phys. Lett.*, 2006, **89**, 122114.
12 Y. Lu, X. W. Li, G. Q. Gong, G. Xiao, A. Gupa, P. Lecoeur, J. Z. Sun, Y. Y. Wang and V. P. Dravid, *Phys. Rev. B: Condens. Matter Mater. Phys.*, 1996, **54**, R8357.
13 Z. H. Xiong, D. Wu, Z. Valy Vardeny and J. Shi, *Nature*, 2004, **427**, 821.
14 L. E. Hueso, J. M. Pruneda, V. Ferrari, G. Burnell, J. P. Valdes-Herrera, B. D. Simons, P. B. Littlewood, E. Artacho, A. Fert and N. D. Mathur, *Nature*, 2007, **445**, 410.
15 D. Sun, L. Yin, C. Sun, H. Guo, Z. Gai, X. G. Zhang, T. Ward, Z. Cheng and J. Shen, *Phys. Rev. Lett.*, 2010, **104**, 236602.
16 C. Barraud, P. Seneor, R. Mattana, S. Fusil, K. Bouzehouane, C. Deranlot, P. Graziosi, L. Hueso, I. Bergenti, V. Dediu, F. Petroff and A. Fert, *Nat. Phys.*, 2010, **6**, 615.

17 F. Li, T. Li and X. Guo, *ACS Appl. Mater. Interfaces*, 2014, **6**, 1187.

18 F. Wang and Z. V. Vardeny, *Synth. Met.*, 2010, **160**, 210.

19 M. Huijben, L. Martin, Y. H. Chu, M. Holcomb, P. Yu, G. Rijnders, D. Blank and R. Ramesh, *Phys. Rev. B: Condens. Matter Mater. Phys.*, 2008, **78**, 094413.

20 J. H. Song, T. Susaki and H. Y. Hwang, *Adv. Mater.*, 2008, **20**, 2528.

21 J. X. Ma, X. F. Liu, T. Lin, G. Y. Gao, J. P. Zhang, W. B. Wu, X. G. Li and J. Shi, *Phys. Rev. B: Condens. Matter Mater. Phys.*, 2009, **79**, 174424.

22 M. Cesaria, A. P. Caricato, G. Maruccio and M. Martino, *J. Phys.: Conf. Ser.*, 2011, **292**, 012003.

23 H. Boschker, M. Huijben, A. Vailionis, J. Verbeeck, S. V. Aert, M. Luysberg, S. Bals, G. V. Tendeloo, E. P. Houwman, G. Koster, D. H. A. Blank and G. Rijnders, *J. Phys. D: Appl. Phys.*, 2011, **44**, 205001.

24 A. M. De Leon-Guevara, P. Berthet, J. Berthon, F. Millot, A. Revcolevschi, A. Anane, C. Dupas, K. Le Dang, J. P. Renard and P. Veillet, *Phys. Rev. B: Condens. Matter Mater. Phys.*, 1997, **56**, 6031.

25 R. Shiozaki, K. Takenaka, Y. Sawaki and S. Sugai, *Phys. Rev. B: Condens. Matter Mater. Phys.*, 2001, **63**, 184419.

26 J. F. Mitchell, D. N. Argyriou, C. D. Potter, D. G. Hinks, J. D. Jorgensen and S. D. Bader, *Phys. Rev. B: Condens. Matter Mater. Phys.*, 1996, **54**, 6172.

27 T. Ohnishi, K. Shibuya, M. Lippmaa, D. Kobayashi, H. Kumigashira, M. Oshima and H. Koinuma, *Appl. Phys. Lett.*, 2004, **85**, 272.

28 W. Yuan, Y. L. Zhao, C. Tang, T. Su, Q. Song, J. Shi and W. Han, *Appl. Phys. Lett.*, 2015, **107**, 022404.

29 M. Huijben, L. W. Martin, Y.-H. Chu, M. B. Holcomb, P. Yu, G. Rijnders, D. H. A. Blank and R. Ramesh, *Phys. Rev. B: Condens. Matter Mater. Phys.*, 2008, **78**, 094413.